

Refining molecular potentials using atom interferometry

Robert C. Forrey,¹ Li You,² Vasili Kharchenko,¹ and Alex Dalgarno¹

¹Institute for Theoretical Atomic and Molecular Physics, Harvard-Smithsonian Center for Astrophysics, 60 Garden Street, Cambridge, Massachusetts 02138

²School of Physics, Georgia Institute of Technology, Atlanta, Georgia 30332-0430

(Received 5 December 1996)

We present a theoretical study of the index of refraction of argon for the propagation of sodium matter waves. The sensitivity of the index of refraction to the details of the molecular potential curve is analyzed. Our calculations reveal velocity-dependent oscillations in the index of refraction that may be detectable, particularly at low temperatures, in atom interferometry measurements. A procedure for refining molecular potential curves is outlined. [S1050-2947(97)50305-2]

PACS number(s): 03.75.Dg, 03.65.Bz, 07.60.Ly

Recently, atom interferometry [1] has been successfully applied to measuring the complex index of refraction for sodium matter waves passing through a noble-gas medium [2,3]. With the application of multiple-scattering theory [4,5] these experiments provide the capability for directly measuring the average forward-scattering amplitude of an atomic collision. It has been suggested [5,6] that this feature provides the possibility for refining molecular potential curves. The motivation for the present work is to provide a bridge between the molecular potential curves obtained from existing spectroscopic data and the index of refraction measurements obtained from present and future atom interferometry experiments.

For the light noble gases He and Ne, it was shown [5] that the index of refraction is sensitive to the “glory” contribution to the forward-scattering amplitude that arises from undeflected classical trajectories. A connection was made between short-range potential parameters and the index of refraction measurements. For heavier systems such as Ar, the glory contribution has also been predicted to be important [6]. However, the argument in [3] that the measurements are most sensitive to the long-range part of the molecular potential applies to heavy systems possessing many bound states. Therefore, the connection between potential parameters and the interpretation of atom interferometry measurements may be different for heavy systems than for light systems. In the present work, we investigate this connection for the case of sodium atoms passing through argon.

For the atom interferometry measurements [3], it has been established [3,5,6] that the noble gas can be treated as an effective medium with a complex index of refraction

$$n(k_L) = 1 + \frac{2\pi N}{k_L} \left\langle \frac{f(k,0)}{k} \right\rangle, \quad (1)$$

where N is the number density of the medium and k_L is the momentum of the beam in the laboratory frame. The forward-scattering amplitude $f(k,0)$ is calculated in the center-of-mass frame for two particles with relative momentum k . Atomic units are assumed unless otherwise indicated. The notation $\langle \dots \rangle$ in Eq. (1) refers to a statistical average

with respect to all microscopic parameters of the medium. Following [5], we average with respect to the momentum distribution

$$\begin{aligned} p(k) = & (m_T + m_P) \sqrt{\frac{\beta}{\pi m_T m_P E}} \sinh \left(\frac{\beta m_T k}{\mu} \sqrt{\frac{2E}{m_P}} \right) \\ & \times \exp \left\{ -\beta \left[\frac{k^2}{2\mu} \left(1 + \frac{m_T}{m_P} \right) + E \left(\frac{m_T}{m_P} \right) \right] \right\}, \end{aligned} \quad (2)$$

where μ is the reduced mass $m_T m_P / (m_T + m_P)$ with m_P and m_T the respective masses of the projectile and target atoms, $E = k_L^2 / 2m_P$ is the kinetic energy of the projectile atom, and β is the inverse of the Boltzmann constant times the temperature. The statistical procedure given above is different from the one used by Vigue and co-workers [6] in that a distinction is made between the laboratory momentum k_L and the relative momentum k . This difference may become significant for applications where the distribution of projectile velocities is wide compared to the spread in target velocities, or when the projectile velocity is much smaller than the average relative velocity of collision, i.e., $k_L \ll \sqrt{\mu/\beta}$. In the experiment of Schmiedmayer *et al.* [3], the sodium matter wave has a velocity width that is only a few percent of the peak k_L . The relative velocity distribution is much wider, so we can neglect the average over projectile velocities, and the difference between the distributions used in [5] and [6] is negligible.

The forward-scattering amplitude is calculated from the molecular potential $V(r)$ between the sodium and argon atoms. The potential scattering calculations are performed using both the standard quantum partial-wave theory and the semiclassical eikonal approximation. In the quantum calculation, the scattering amplitude is obtained from the expansion

$$f(k, \theta) = \frac{1}{2ik} \sum_{l=0}^{\infty} (2l+1) [\exp(2i\delta_l) - 1] P_l(\cos\theta), \quad (3)$$

where δ_l is the numerically computed phase shift and θ is the center-of-mass scattering angle. In the eikonal approximation, the scattering amplitude is given by

$$f(k,0) = -ik \int_0^\infty \{\exp[2i\eta(b)] - 1\} b db, \quad (4)$$

where b is the classical impact parameter and $\eta(b)$ is the corresponding phase shift function

$$\eta(b) = -\frac{1}{4k} \int_{-\infty}^{+\infty} U(b,z) dz, \quad (5)$$

with

$$U(b,z) = 2\mu V(\sqrt{b^2 + z^2}). \quad (6)$$

The NaAr potential can be represented in terms of a short-range part V_S and long-range part V_L ,

$$V(r) = \begin{cases} V_S(r), & r < r_m \\ V_L(r), & r > r_m \end{cases} \quad (7)$$

where

$$V_S(r) = D_e [e^{-2a(r-r_0)} - 2e^{-a(r-r_0)}] + \Delta, \quad (8)$$

$$V_L(r) = -C_6 g_6(b;r) - C_8 g_8(b;r) - C_{10} g_{10}(b;r). \quad (9)$$

The parameters a , D_e , and r_0 are the standard Morse potential parameters and r_m is a matching radius. The constant Δ is a small offset, similar to the one used by Vigue and co-workers [6], that can be used together with the functions $g_n(b;r)$ to smooth the connection between the short- and long-range potentials. With the definitions

$$g_n(b;r) = \frac{\gamma(n,br)}{(n-1)!r^n}, \quad (10)$$

$$\gamma(n,br) = (n-1)! \left[1 - \exp(-br) \sum_{m=0}^{n-1} \frac{(br)^m}{m!} \right], \quad (11)$$

we obtain as $r \rightarrow \infty$, the van der Waals expansion

$$V_L(r) \sim -\frac{C_6}{r^6} - \frac{C_8}{r^8} - \frac{C_{10}}{r^{10}}. \quad (12)$$

To determine the parameters for our short-range Morse potential, we used the measurements of Smalley *et al.* [7] and Pritchard [8]. The long-range van der Waals coefficients are taken from [9]. We require the potential and its derivative to be continuous at the matching point r_m . The values of Δ , r_m , and b are obtained by a least-squares fit to this requirement. Our procedure offers a slight improvement over the approach used by Vigue and co-workers [6], which does not constrain the potential derivative to be continuous at r_m . The potential parameters are given in Table I. Figure 1 shows logarithmic and linear plots of the interaction potential with and without the long-range tail.

We have calculated the ratio of the real to the imaginary part of the forward-scattering amplitude in the center-of-mass frame for the NaAr potential

$$R(k) \equiv \frac{\text{Re}[f(k,0)]}{\text{Im}[f(k,0)]}. \quad (13)$$

TABLE I. Potential parameters.

Parameter	Value	Units
a	0.498 895 6	a.u.
b	1.268 26	a.u.
D_e	45.43	cm ⁻¹
Δ	-0.325	cm ⁻¹
r_0	4.991	Å
r_m	10.2672	Å
C_6	190	a.u.
C_8	12 700	a.u.
C_{10}	820 000	a.u.

In Fig. 2, we compare the quantum calculation with the eikonal calculation. The agreement between the two calculations is very good for $k > 25$. Several thousand partial waves are required for the quantum calculation to converge when $k > 25$, so we use the eikonal approximation for large values of k .

Oscillatory structure appears in both the quantum and eikonal calculations. The narrow structures that occur in the quantum calculation at low values of k are shape resonances. The eikonal calculation oscillates near the value 0.72, which is what is obtained when only the long-range potential is used [3]. The phase of the eikonal oscillation is given by [10,11]

$$\phi_E = 2 \left[\eta(b_g) - \frac{3\pi}{8} \right] \quad (14)$$

where the “glory” impact parameter b_g is evaluated from the condition

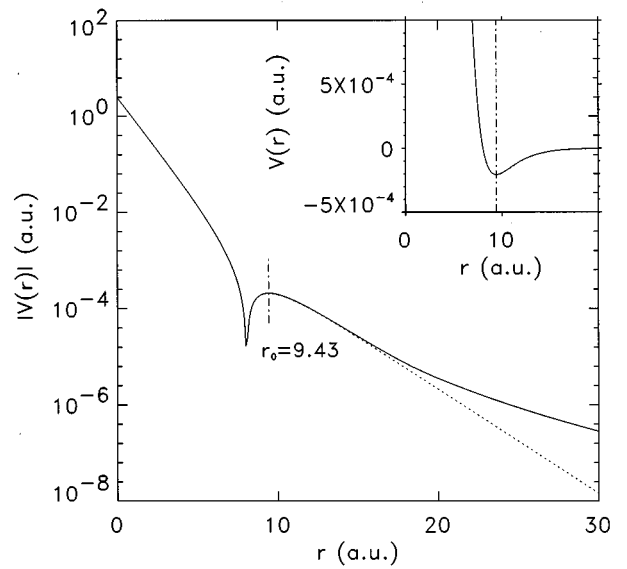


FIG. 1. The absolute value of the NaAr interaction potentials. The solid curve is for the Morse potential connected to a long-range van der Waals expansion. The dashed curve is for the Morse potential. The inset shows the potentials on a linear scale; there is no discernible difference between the two curves.

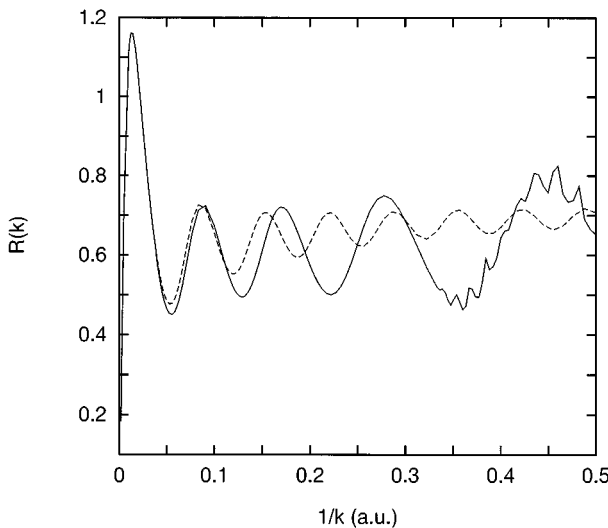


FIG. 2. The ratio $R(k)$ versus $1/k$. The solid curve is the quantum calculation and the dashed curve is the eikonal calculation.

$$\left. \frac{d\eta(b)}{db} \right|_{b=b_g} = 0. \quad (15)$$

The glory impact parameter changes with energy, so it is possible to define a trajectory $b_g \equiv b_g(k)$ that describes the evolution of ϕ_E with k . A quantum phase function ϕ_Q can be similarly defined to be the largest δ_i for a given k . The eikonal calculations demonstrate that ϕ_E is proportional to $1/k$, while the quantum calculations show that $\phi_Q \leq \phi_E$ with strong deviations from the $1/k$ proportionality when k is small.

In order to study the importance of the long-range part of the potential, we performed calculations using the Morse potential with and without the van der Waals contribution. Figure 3 compares the two calculations of $R(k)$ over a wide range of energies. For $k > 1$ a.u. the phase ϕ_Q is nearly the

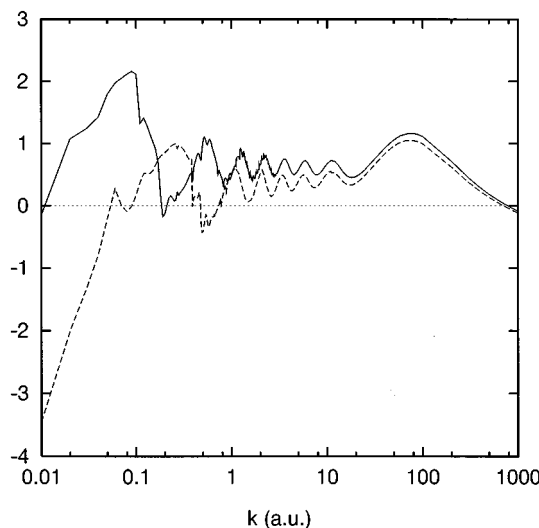


FIG. 3. The ratio $R(k)$ versus k . The solid curve is for the Morse potential connected to a long-range van der Waals expansion. The dashed curve is for the Morse potential.

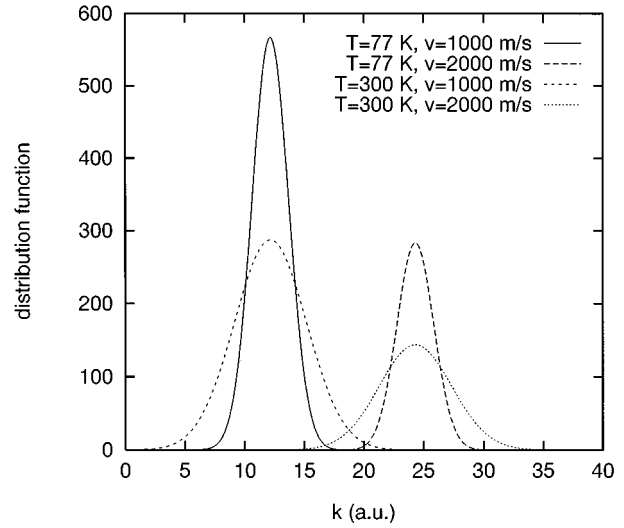


FIG. 4. The NaAr relative momentum distribution function. The four plots correspond to sodium projectile velocities of 1000 and 2000 m/s, and argon gas temperatures of 77 and 300 K.

same for both calculations, which suggests that long range scattering regulates the amplitude, and glory scattering regulates the phase of $R(k)$ when k is sufficiently large.

The total variation of the quantum phase is

$$\Delta\phi_Q = \phi_Q|_{k=0} - \phi_Q|_{k=\infty} = 2\pi n, \quad (16)$$

where n is the number of rotationless bound states that are supported by the molecular potential [10,11]. For a Morse potential, the number of bound states is known analytically [12],

$$n = \text{Int}\left[\frac{1}{a}\sqrt{2\mu D_e} - \frac{1}{2}\right] + 1. \quad (17)$$

For the Morse potential in Fig. 1, there are seven bound states, and for the full NaAr potential of Fig. 1, there are eight. Counting the number of coarse oscillations in Fig. 3 yields the correct number of bound states for both potentials.

The $k \rightarrow 0$ limiting behavior of the ratio of the real to the imaginary part of the scattering amplitude can be used to determine the parameters of the effective range expansion

$$R(k) \sim -(a_s k)^{-1} + \frac{1}{2} r_e k, \quad (18)$$

where a_s is the scattering length and r_e is the effective range of the potential. For the full NaAr potential of Fig. 1, the values of a_s and r_e are 170 and 20 a.u., respectively. The accuracy of these estimates is very sensitive to the long-range tail of the potential. Therefore, atom interferometry could potentially play an important role in determining better effective range parameters.

Thermal averaging is needed to get the ratio of the real to the imaginary part of the forward-scattering amplitude in the laboratory frame where the effective medium is defined. Figure 4 is a plot of the distribution function (2) for sodium

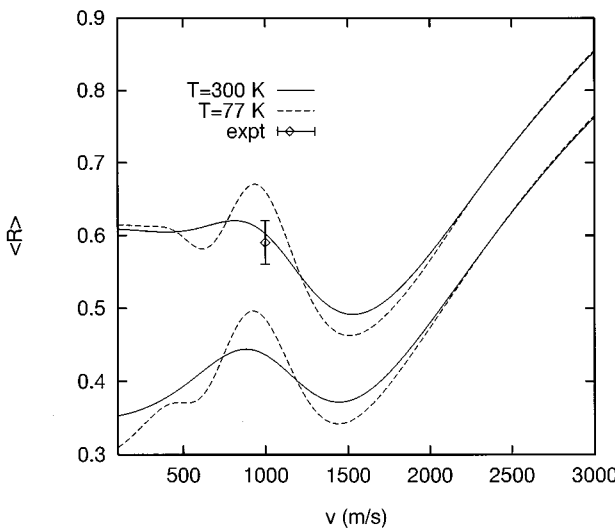


FIG. 5. The thermally averaged ratio R as a function of projectile velocity for argon gas temperatures of 77 and 300 K. The upper curves are for the Morse potential connected to the long-range van der Waals expansion. The lower curves are for the Morse potential. Also shown is the measurement of Schmiedmayer *et al.* (Ref. [3]).

projectile velocities v and argon gas temperatures T that are being considered in future experiments [8]. The spread is widest for high temperatures.

Figure 5 shows the velocity dependence of the ratio of the real to the imaginary part of the forward-scattering amplitude in the laboratory frame for $T=300$ K and $T=77$ K. For $T=300$ K, the thermal averaging tends to suppress the glory oscillations when converted to the laboratory frame. At $T=77$ K, the glory oscillations become more prominent. For both temperatures, the shape resonance structure tends to be washed out by thermal averaging. Also shown in Fig. 5 is the $T=300$ K measurement of Schmiedmayer *et al.* [3]. The agreement between theory and experiment is within experimental uncertainty.

An interpretation presented in [3] indicates that index of refraction measurements are most sensitive to the long-range part of the interatomic potential. For the light noble gases He and Ne, it was shown [5] that the index of refraction is sensitive to the “glory” contribution to the forward-scattering amplitude. A connection was made between short-range po-

tential parameters, such as the position and depth of the potential well, and the index of refraction measurements. In the present work, we have presented a general approach that can be used to interpret the index of refraction measurements for a variety of experimental conditions. The long-range contribution is larger for Ar than for He and Ne, and effectively determines the index of refraction [3]. Nevertheless, velocity-dependent glory oscillations should still be detectable in the index of refraction measurements, particularly at low temperatures where the effect of thermal averaging is reduced.

Vigue [6] has noted that atom interferometry measurements may provide the capability for determining the magnitude and sign of the scattering length for an ultracold gas. For such systems, the relative velocity of collision is very nearly equal to the laboratory velocity, and the scattering length a_s can be approximated by

$$a_s \approx -\lim_{k_L \rightarrow 0} \frac{1}{k_L} \frac{\text{Im}[n(k_L)]}{\text{Re}[n(k_L)-1]}. \quad (19)$$

From a theoretical point of view, low-temperature atom interferometry would provide perhaps the most interesting information. The quantum phase function ϕ_Q is quite sensitive to the details of the molecular potential, and its variation is related to the number of bound states of zero angular momentum contained in the potential. If the effect of thermal averaging can be minimized, then ϕ_Q can be resolved and analyzed. By calculating the forward-scattering amplitude with and without the long-range potential tail, and comparing to index of refraction measurements, we can determine which part of the molecular potential is most uncertain. With accurate short-range information, such as the Morse parameters used in the present work, and additional atom interferometry measurements, it would be possible to refine the potential at intermediate to large distances.

We thank David Pritchard and members of his MIT atom interferometer group for helpful discussions. This work was supported by the U.S. Department of Energy, Division of Chemical Sciences, Office of Basic Energy Sciences, Office of Energy Research, and by the National Science Foundation through a grant for the Institute for Theoretical Atomic and Molecular Physics at Harvard University and Smithsonian Astrophysical Observatory.

-
- [1] For a recent review, see *Atom Interferometry*, edited by P. Berman (Academic Press, New York, 1997).
 - [2] D. W. Keith, C. R. Ekstrom, Q. A. Turchette, and D. E. Pritchard, Phys. Rev. Lett. **66**, 2693 (1991).
 - [3] J. Schmiedmayer, M. S. Chapman, C. R. Ekstrom, T. D. Hammond, S. T. Wehinger, and D. E. Pritchard, Phys. Rev. Lett. **74**, 1043 (1995).
 - [4] M. Lax, Rev. Mod. Phys. **23**, 287 (1951).
 - [5] R. C. Forrey, L. You, V. Kharchenko, and A. Dalgarno, Phys. Rev. A **54**, 2180 (1996).
 - [6] J. Vigue, Phys. Rev. A **52**, 3973 (1995); E. Audouard, P. Duplaia, and J. Vigue, Europhys. Lett. **32**, 397 (1995).
 - [7] R. E. Smalley, D. A. Auerbach, P. S. H. Fitch, D. H. Levy, and L. Wharton, J. Chem. Phys. **66**, 3778 (1977).
 - [8] D. E. Pritchard (private communication).
 - [9] A. A. Radzig and B. M. Smirnov, *Reference Data on Atoms, Molecules, and Ions* (Springer-Verlag, Berlin, 1985).
 - [10] R. B. Bernstein, J. Chem. Phys. **38**, 2599 (1963).
 - [11] M. S. Child, *Molecular Collision Theory* (Academic Press, London, 1974).
 - [12] P. M. Morse, Phys. Rev. **34**, 57 (1929).